Fully Enclosed Triboelectric Nanogenerators for Applications in Water and Harsh Environments

*Ya Yang, Hulin Zhang, Ruoyu Liu, Xiaonan Wen, Te-Chien Hou, and Zhong Lin Wang**

With the growing threat of energy crises, new technologies for harvesting wasted ambient mechanical energy are becoming one of the most important fields of research.[1] Currently, there are three physical effects used for harvesting small scale mechanical energy: electromagnetic,[2,3] piezoelectric,[4,5] and triboelectric effects.[6,7] In parallel to the development of micro-/nanopower sources, it is necessary to explore the possibility of harvesting large-scale ambient mechanical energy, such as ocean waves and natural wind.[8] Such energy is abundant and has much less dependence on season, day or night, and the weather than solar energy does. Moreover, the mechanical energy generated by human motion, such as walking or shaking, is usually wasted.[9] Harvesting this kind of energy has potential for powering portable electronic devices.

Triboelectric nanogenerators (TENGs) fabricated using the polymer-polymer or polymer-metal film materials have been extensively developed to power some small electronic devices (such as liquid crystal displays (LCDs) and light-emitting diodes (LEDs)).[10,11] The mechanism is based on the triboelectric effect,[12] in which cycled contact-separation between two different triboelectric materials can induce a voltage drop for driving electrons to flow in the external circuit. Although many kinds of TENGs have been fabricated,[13,14] they are based on a working process with the acting surfaces being exposed to ambient atmosphere, which can limit their applications in some cases. It has been reported that the ambient environment such as humidity can largely weaken the triboelectric effect,[15] so that the fabricated TENGs cannot work under harsh conditions with the presence of water. To solve this problem, it is necessary to develop fully enclosed or packaged TENGs that can tolerate the environment in which they will be employed.

Here, we have demonstrated the first fully enclosed TENGs, which can be used to harvest the wave and biomechanical energies. A TENG was fabricated by using the polytetrafluoroethylene (PTFE)-polyamide (PA) film materials in an enclosed sphere, which can be used to harvest the wave energy from water for driving electronic devices. Two TENGs in an enclosed cylinder can be used to directly light up 60 green LEDs by moving the mass rod at the center of the cylinder; this has potential applications for harvesting the wave and biomechanical energies. The energies produced by the TENGs can be stored in a Li-ion battery for driving an ascorbic acid (AA) biosensor.

Figure 1a shows a schematic diagram of a conventional TENG, which consists of a Cu film as the top electrode, a PTFE film, a PA film, and a Cu film as the bottom electrode. The TENG was driven by a homemade force loading system with the working frequency of 1 Hz. Figure 1b shows the output performance of the fabricated TENG in air, where the open-circuit voltage (V_{oc}) and the short-circuit current (I_{sc}) were about 50 V and 14 μA under the forward connection to the measurement system, respectively. The corresponding V_{oc} and I_{sc} under the reversed connection to the measurement system are shown in Figure S1 (Supporting Information), which are consistent with the results in Figure 1b. The time constants of the output voltage and current peaks are different because the loading resistance is up to 100 MΩ for the voltage measurement and the effective resistance is about several Ohms for the current measurement. Figure 1c shows the output performance of the same TENG in water, indicating that there was no observed output voltage or current signal if the water infiltrated into the TENG.

An optical image of the fabricated device is shown in **Figure 2**a. Figure S2 (Supporting Information) shows a schematic diagram of the device. When the two spheres were periodically in contact and separation, the output voltage and current were observed, as shown in Figure 2b. The TENG was driven by the hand movement in air. The measured largest V_{oc} and I_{sc} are 100 V and 7 μA, respectively.

The mechanism of the TENG is based on the triboelectric effect induced electrostatic charges on the surface of the PTFE and PA films. When the PTFE film is in contact with the PA film, the surface charges are transferred from PA to PTFE due to the different triboelectric polarities,[16] resulting in net negative charges at the PTFE surface and net positive charges at the PA surface, as shown in Figure 2c. Once the two polymers are separated by a gap, electrons are driven to flow from the Cu electrode of PTFE to the Cu electrode of PA to balance the triboelectric charge induced potential, as shown in Figure 2d. This process produces an instantaneous current signal as shown in Figure 2b. When a balance is reached between the potential produced by the induced charges and the triboelectric charges, there is no observed output current signal, as shown in Figure 2e. When the PA film approaches the PTFE film, the potential from the triboelectric charges drops, thus the electrons in the Cu electrode of PA flow back to the Cu electrode of PTFE (Figure 2f), resulting in an opposite current signal. When the two polymers are in contact again, the potential

Dr. Y. Yang, H. Zhang, R. Liu, X. Wen, T.-C. Hou, Prof. Z. L. Wang
School of Materials Science and Engineering
Georgia Institute of Technology
Atlanta, GA 30332, USA
E-mail: zlwang@gatech.edu
Prof. Z. L. Wang
Beijing Institute of Nanoenergy and Nanosystems
Chinese Academy of Sciences
Beijing, China

DOI: 10.1002/aenm.201300376

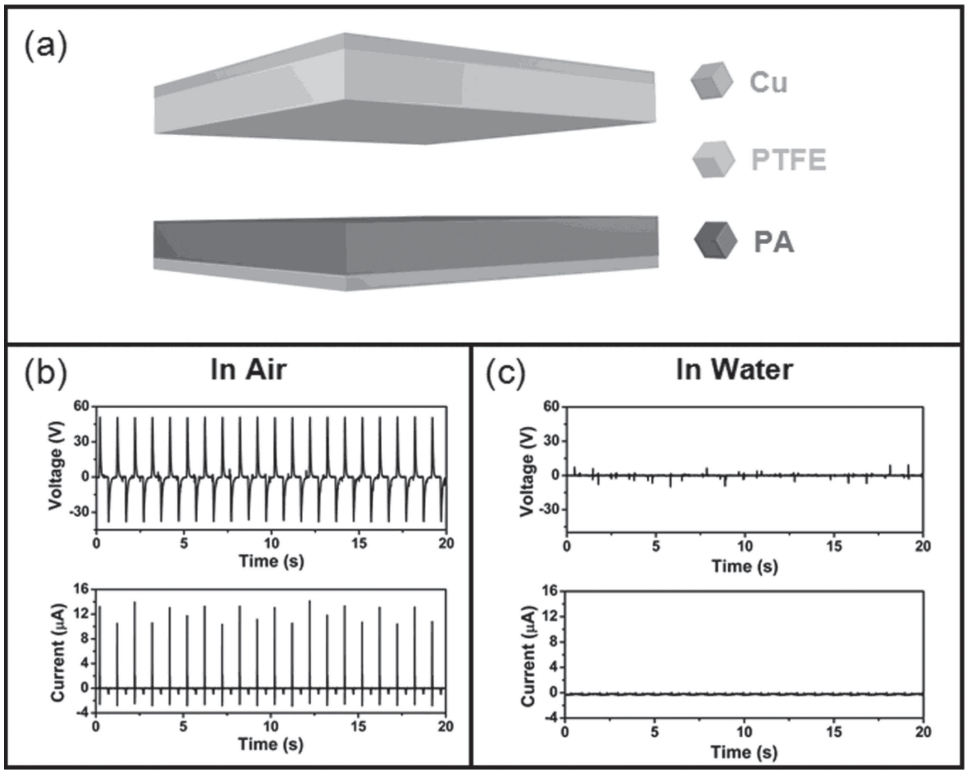

Figure 1. a) Schematic diagram of the fabricated conventional TENG without packaging using two insulator materials. b) Measured output voltage and current of the TENG in air. c) Measured output voltage and current of the TENG emerged in water.

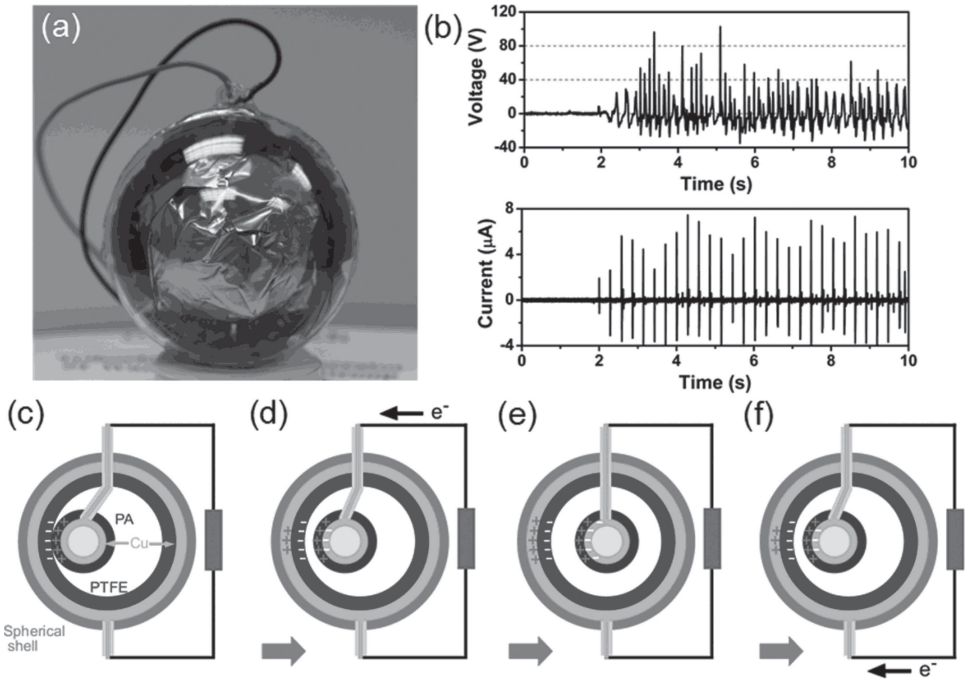

Figure 2. a) Photograph of the fabricated TENG in a fully enclosed spherical shell. b) Measured output voltage and current the TENG when it was shaken by hand. c–f) Sketches that illustrate the operating principle of the TENG.

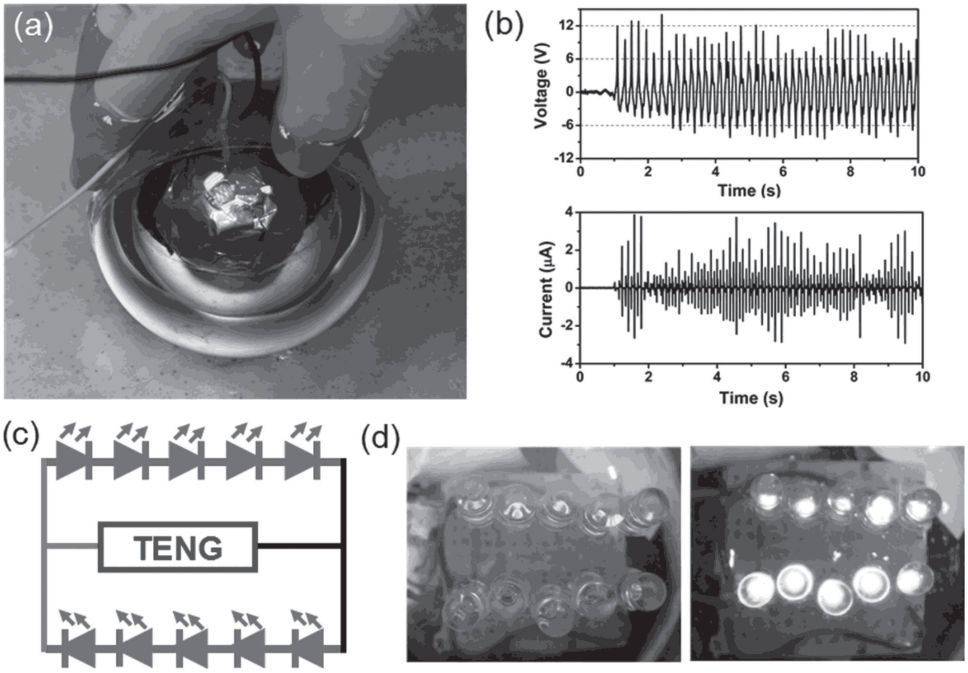

Figure 3. a) Photograph of the fabricated TENG in a fully enclosed spherical shell in water. b) Measured output voltage and current the TENG in a. c) Schematic diagram of the connection between the TENG and 10 green LEDs. d) Optical images of 10 green LEDs in water before and after being driven by the TENG.

drop created by the triboelectric charges reaches minimum, as shown in Figure 2c.

Figure 3a shows an optical image of the fabricated TENG in the enclosed spherical shell in water. When the PTFE and PA films were contacted and separated in water, the corresponding V_{oc} and I_{sc} of the TENG are about 12 V and 4 μA (Figure 3b), respectively. It indicates that the designed TENG can work in water for harvesting wave energy. The smaller output performance for the TENG in water is due to the smaller movement amplitude of the TENG in water than that in air. To confirm that the produced energy in water can be used to drive some electronic devices in water, 10 green LEDs were connected with the TENG, as shown in Figure 3c. Both the TENG and the LEDs were put into the water. Figure 3d shows the optical images of the 10 green LEDs, which were directly lit up by the TENG in water. The movie file 1 (Supporting Information) also shows how to use the TENG to drive 10 green LEDs in water by harvesting the wave energy.

In this study, the output voltage V_{oc} of TENG is approximately given by

$$V_{oc} = \frac{\sigma d}{\varepsilon_0} \quad (1)$$

where σ is the triboelectric charge density, d is the interlayer distance, and ε_0 is the permittivity in vacuum.[17] According to Equation 1, the output voltage V_{oc} will increase with increasing the interlayer distance d. The output current I_{sc} of TENG is associated with the changing speed of the interlayer distance. The faster changing speed can result in a larger output current. To enhance the output performance of the enclosed TENG, we designed another structure for a TENG. **Figure 4**a shows an optical image and the corresponding schematic diagram of the TENGs in an enclosed cylinder/tube. Both the top and bottom TENGs consist of a Cu film electrode, a PA film, a PTFE film, and another Cu film electrode. A mass rod was placed at the center of the cylinder. When the rod was moved up and down, both the TENGs can be used to harvest mechanical energy. Figure 4b,c show the output performances of the top and bottom TENGs when the rod was moved up and down in the cylinder, respectively. It can be clearly seen that the largest V_{oc} and I_{sc} are about 260 V and 40 μA (Figure 4c), respectively. The total output voltage and current of the TENG when the top and bottom TENGs were connected in parallel is shown in Figure 4d.

Figure 5 shows the working mechanism of the TENGs when a rod was moved up and down in the cylinder. At original state, there was no triboelectric or induced charges in the system, as shown in Figure 5a. No output voltage or current can be observed. We now use the TENG2 at the bottom as an example to illustrate the working mechanism, and the TENG1 at the top is by the same token. When the PTFE-2 and PA-2 films were brought into contact with each other at the bottom of the cylinder (Figure 5b), electrons were injected from PA-2 to PTFE-2 due to the different triboelectric polarities. Thus, the net negative and positive charges were induced at the PTFE-2 and PA-2 surfaces, respectively. These triboelectric charges have a long-time retention in the respective films due to the insulating property of the polymers.[18] When the rod was moved upwards, the electrons flowed from the Cu electrode of the PTFE-2 film to the Cu electrode of the PA-2 film to balance the potential created by the triboelectric charges, resulting in the output current signals (Figure 5c). When the rod was moved down (Figure 5c), the electrons were returned from the Cu electrode of PA-2 to the Cu electrode of PTFE-2,

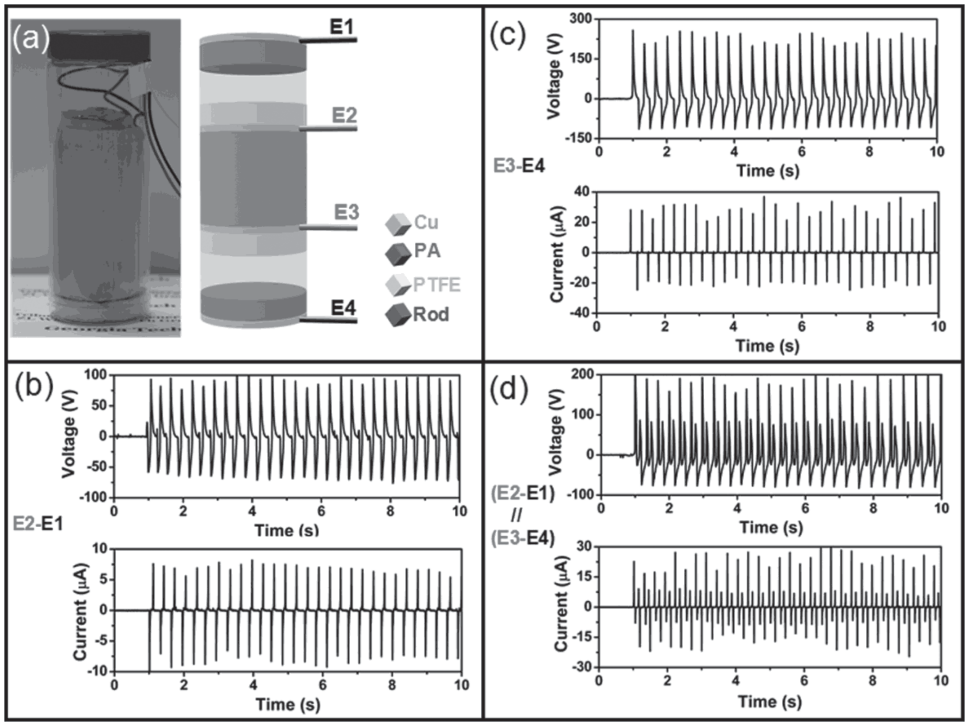

Figure 4. a) Photograph and schematic diagram of the fabricated TENGs in a fully enclosed cylinder. b) Measured output voltage and current of the TENG at the top of the cylinder. c) Measured output voltage and current of the TENG at the bottom of the cylinder. d) Measured output voltage and current of the two TENGs connected in parallel.

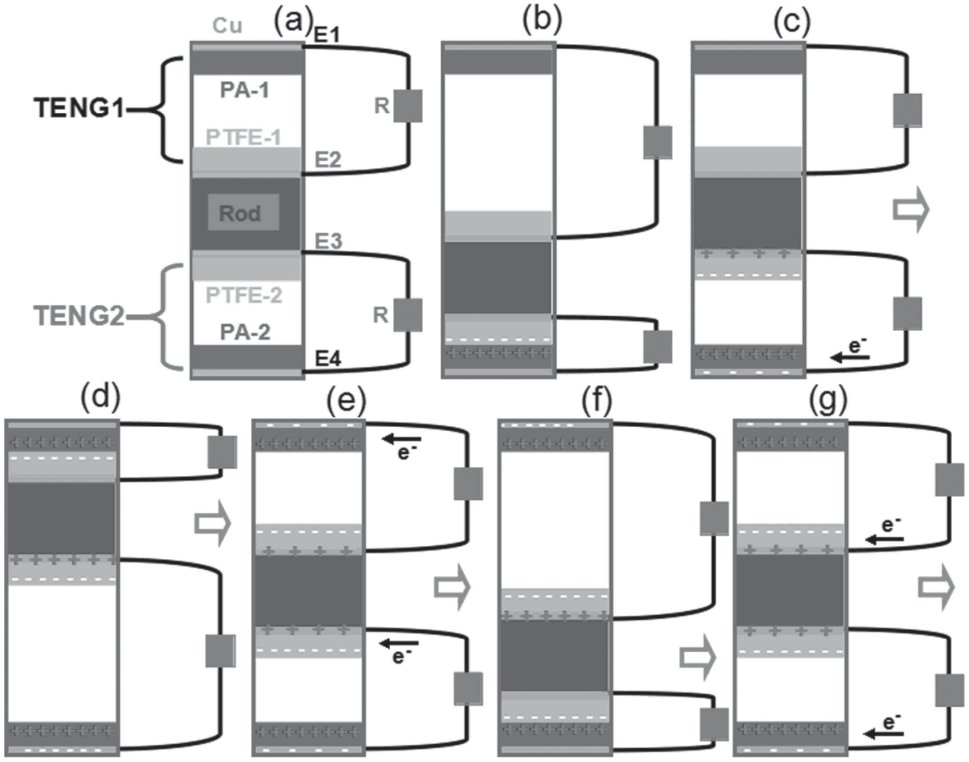

Figure 5. a–g) Sketches that illustrate the operating principle of the TENGs in the enclosed cylinder.

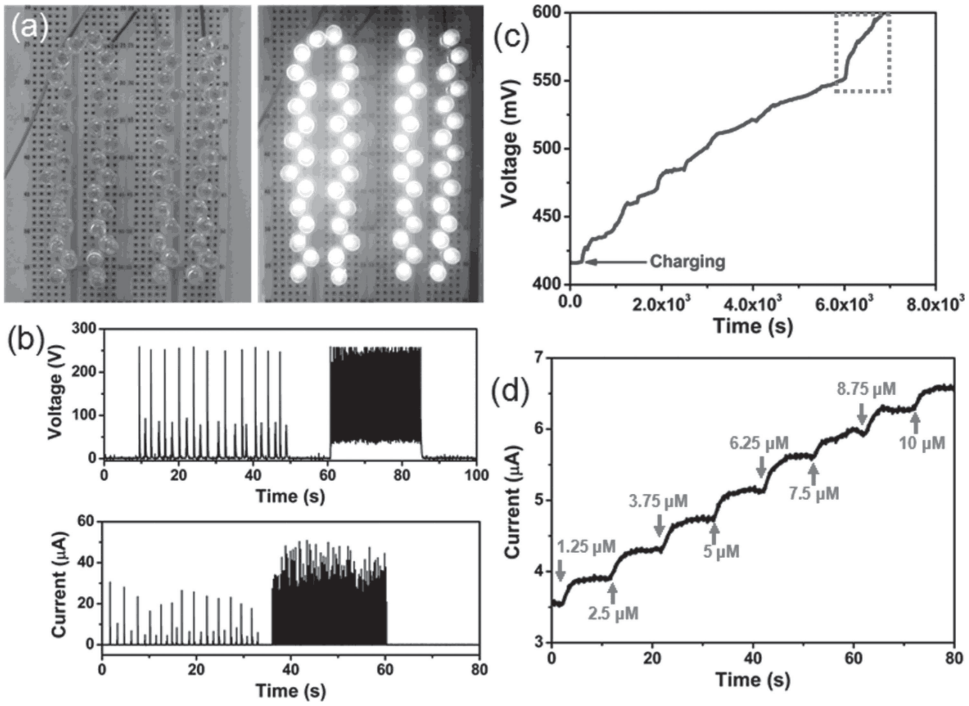

Figure 6. a) Optical images of 60 green LEDs before (left) and after (right) being lighted up by the TENGs. b) Rectified output voltage and current of the TENGs. c) The TENG charging curve of a Li-ion battery. d) Current response of the fabricated biosensor to the AA solution with different concentrations.

resulting in a negative current. When the PA-2 film was in contact with the PTFE-2 film at the bottom of the cylinder, there was no observed output current, as shown in Figure 5f. When the rod was moved up again (Figure 5g), electrons flowed from the electrode of PTFE-2 to the electrode of PA-2, resulting in a positive current. This is the process for generating the AC output signals. The TENG1 at the top works in the same way as TENG2 except with a 180° shift in output signals.

To illustrate the potential applications of the fabricated TENGs, we demonstrated that the energy produced by the TENGs can be directly used to light 60 green LEDs or can be stored in a Li-ion battery for driving biosensors. **Figure 6**a shows optical images of the 60 green LEDs before and after being lighted up by the TENGs, which are also shown in the movie file 2 (Supporting Information). To charge a Li-ion battery, a bridge rectification circuit was used to convert the alternating current signals into the direct current signals. Figure 6b shows the rectified output voltage and current of the TENGs under the slow and fast movement of the rod in the cylinder. It can be clearly seen that the increase in the rod movement speed can effectively increase the output current. The largest output voltage and current are about 260 V and 50 μA, respectively. The enlarged output voltage and current curves are shown in Figure S3 (Supporting Information), indicating that both the top (marked with red circle) and bottom TENGs are working. Figure 6c shows that a Li-ion battery was charged by the TENGs from 416 mV to 600 mV by continuously moving the rod in the cylinder several thousand times. Compared with the beginning section of the charging curve, the faster increase of the charging voltage (marked with a dashed rectangle) is due to the faster movement of the rod, which is consistent with the enhanced current in Figure 5b.

In this study, we used a graphite electrode as the sensitive electrode material for detecting the AA molecules. Figure 6d shows the current response to the continuous addition of AA molecules as driven by a TENG charged Li-ion battery of about 0.6 V (Figure 6c). It can be clearly seen that the detection limit of the fabricated sensor is about 1.25 μM and the current response increases with increasing the detected concentration of the AA molecules in PBS. The reaction mechanism of AA molecules is based on the redox reaction occurred on the electrodes,[19] which has a contribution to the increase of the current in Figure 6d. Figure S4 (Supporting Information) shows the plot of the response current density versus the AA solution concentration in PBS, indicating a linear response of the sensor to AA concentration.

In summary, we have demonstrated two possible designs for fully enclosed TENGs for application in the presence of water. By using the PTFE and PA films, the fabricated TENG in an enclosed spherical shell can be used to harvest the wave energy for driving electronic devices in water. Two TENGs were fabricated in an enclosed cylinder, which can be used to harvest wave and biomechanical energies by shaking the rod at the center of the cylinder. The energy produced by TENGs can be used to directly light 60 green LEDs or to charge a Li-ion battery for driving an AA biosensor. The fully enclosed TENGs have potential applications in driving electronic devices and biosensors in air and water.

Experimental Section

Fabrication of the TENGs in an Enclosed Sphere/Sylinder: For the TENG in an enclosed spherical shell, a Cu film (250 nm) electrode was

evaporated on a PTFE film (thickness of 25 μm), which was attached to the inner surface of a large transparent plastic ball (diameter of 80 mm). Moreover, another Cu film (250 nm) was evaporated on a PA film (thickness of 25 μm), which was attached to the outer surface of a smaller sphere (diameter of 50 mm). The smaller sphere was placed inside the large spherical shell, and both are linked by the cables. The fabricated device was then sealed with epoxy paint so that it is fully waterproof. The fabricated TENG was based on the contact-separation between the PTFE film on the inner surface of the larger spherical shell and the PA film on the outer surface of the smaller sphere to induce a voltage drop for driving electrons to flow in the external circuit. The smaller sphere could freely oscillate in any direction in responding to the disturbance from the environment. For the TENGs in an enclosed cylinder, two PA films with the Cu film electrodes were fixed on the top and bottom inside surfaces of the cylinder (length of 180 mm, diameter of 65 mm), respectively. A cylindrical rod was placed inside the cylinder, the top and bottom end surfaces of which were covered by the PTFE films with the Cu film electrodes. Two TENGs were fabricated at the top and bottom inside surfaces of the cylinder, respectively, and they could work alternately when the rod was shaken up and down inside the cylinder.

Measurement of the TENGs and the AA Biosensor: The output voltage of the NGs was measured using a low-noise voltage preamplifier (Keithley 6514 System Electrometer). The output current of the NGs was measured with a low-noise current preamplifier (Stanford Research SR560). The performance of the Li-ion battery was measured using a battery analyzer (MTI Corporation). For the AA biosensor, a platinum electrode and a graphite electrode were employed to detect AA molecules in the phosphate buffer solution (PBS) (pH = 7.4) with a concentration of 0.1 M. In the electrochemical reaction, they served as the counter electrode and working electrode, respectively. The graphite electrode was prepared as follows. First, a polished graphite substrate was washed with ethanol and deionized water. Then, a metal wire was pasted on the graphite with ohmic contact with silver paste. Finally, epoxy was used to cover the edges and back of the electrode to create an open area. All experiments were carried out at room temperature.

Supporting Information

Supporting Information is available from the Wiley Online Library or from the author.

Acknowledgements

This work was supported by Airforce, MURI, U.S. Department of Energy, Office of Basic Energy Sciences (DE-FG02–07ER46394), NSF, and the Knowledge Innovation Program of the Chinese Academy of Sciences (KJCX2-YW-M13).

Received: April 7, 2013
Revised: June 7, 2013
Published online: July 16, 2013

[1] Z. L. Wang, W. Wu, *Angew. Chem.* **2012**, *51*, 11700.
[2] T. von Büren, P. D. Mitcheson, T. C. Green, E. M. Yeatman, A. S. Holmes, G. Troster, *IEEE Sens. J.* **2006**, *1*, 28.
[3] C. B. Williams, C. Shearwood, M. A. Harradine, P. H. Mellor, T. S. Birch, R. B. Yates, *IEEE Proc.- Circuits Dev. Syst.* **2001**, *148*, 337.
[4] L. Gu, N. Cui, L. Cheng, Q. Xu, S. Bai, M. Yuan, W. Wu, J. Liu, Y. Zhao, F. Ma, Y. Qin, Z. L. Wang, *Nano Lett.* **2013**, *13*, 91.
[5] K. Park, M. Lee, Y. Liu, S. Moon, G.-T. Hwang, G. Zhu, J. Kim, S. O. Kim, D. K. Kim, Z. L. Wang, *Adv. Mater.* **201 2**, *24*, 2999.
[6] R. Pelrine, R. D. Kornbluh, J. Eckerle, P. Jeuck, S. Oh, Q. Pei, S. Stanford, *Proc. SPIE* **2001**, *4329*, 148.
[7] F.-R. Fan, Z.-Q. Tian, Z. L. Wang, *Nano Energy* **2012**, *1*, 328.
[8] J. Falnes, *Mar. Struct.* **2007**, *20*, 185.
[9] L. C. Rome, L. Flynn, E. M. Goldman, T. D. Yoo, *Science* **2005**, *309*, 1725.
[10] Z. Guang, C. Pan, W. Guo, C.-Y. Chen, Y. Zhou, R. Yu, Z. L. Wang, *Nano Lett.* **2012**, *12*, 4960.
[11] Y. Yang, H. Zhang, S. Lee, D. Kim, W. Hwang, Z. L. Wang, *Nano Lett.* **2013**, *13*, 803.
[12] F.-R. Fan, L. Long, G. Zhu, W. Wu, R. Zhang, Z. L. Wang, *Nano Lett.* **2012**, *12*, 3109.
[13] X.-S. Zhang, M.-D. Han, R.-X. Wang, F.-Y. Zhu, Z.-H. Li, W. Wang, H.-X. Zhang, *Nano Lett.* **2013**, *13*, 1168.
[14] J. Zhong, Q. Zhong, F. Fan, Y. Zhang, S. Wang, B. Hu, Z. L. Wang, J. Zhou, *Nano Energy* **2013**, DOI: 10.1016/j.nanoen.2012.11.015.
[15] E. Nemeth, V. Albrecht, G. Schubert, F. Simon, *J. Electrostat.* **2003**, *58*, 3.
[16] J. A. Cross, *Electrostatics: Principles, Problems and Applications*, Adam Hilger, Bristol **1987**, Ch. 2.
[17] Y. Yang, L. Lin, Y. Zhang, Q. Jing, T.-C. Hou, Z. L. Wang, *ACS Nano* **2012**, *6*, 10378.
[18] F. Saurenbach, D. Wollmann, B. D. Terris, A. F. Diaz, *Langmuir* **1992**, *8*, 1199.
[19] X. Wang, C. Hu, H. Liu, G. Du, X. He, Y. Xi, *Sens. Actuators B* **2010**, *144*, 220.